

# Mask2Former for Video Instance Segmentation

B. Cheng<sup>1,2</sup>  A. Choudhuri<sup>1</sup> I. Misra<sup>2</sup> A. Kirillov<sup>2</sup> R. Girdhar<sup>2†</sup> A. G. Schwing<sup>1†</sup>

<sup>1</sup>University of Illinois at Urbana-Champaign (UIUC) <sup>2</sup>Facebook AI Research (FAIR)

<https://github.com/facebookresearch/Mask2Former>

## Abstract

We find Mask2Former [4] also achieves state-of-the-art performance on video instance segmentation without modifying the architecture, the loss or even the training pipeline. In this report, we show universal image segmentation architectures trivially generalize to video segmentation by directly predicting 3D segmentation volumes. Specifically, Mask2Former sets a new state-of-the-art of 60.4 AP on YouTubeVIS-2019 and 52.6 AP on YouTubeVIS-2021. We believe Mask2Former is also capable of handling video semantic and panoptic segmentation, given its versatility in image segmentation. We hope this will make state-of-the-art video segmentation research more accessible and bring more attention to designing universal image and video segmentation architectures.

## 1. Introduction

Video instance segmentation [18] differs from image segmentation in its goal to simultaneously segment and track objects in videos. Initial methods [14, 18] add “track embeddings” to per-pixel image segmentation architectures to track objects across time. Recent transformer-based methods [8, 15, 16] use “object queries” [2] to connect objects across frames. However, all these methods are specifically designed to only process video data, disconnecting image and video segmentation research.

Universal image segmentation methods [4, 5] show that mask classification is able to address common image segmentation tasks (*i.e.* panoptic, instance and semantic) using the same architecture, and achieve state-of-the-art results. A natural question emerges: does this universality extend to videos? In this report, we find Mask2Former [4] achieves state-of-the-art results on video instance segmentation as well *without* modifying the architecture, the loss or even the training pipeline. To achieve this, we let Mask2Former directly attend to the 3D spatio-temporal features and pre-

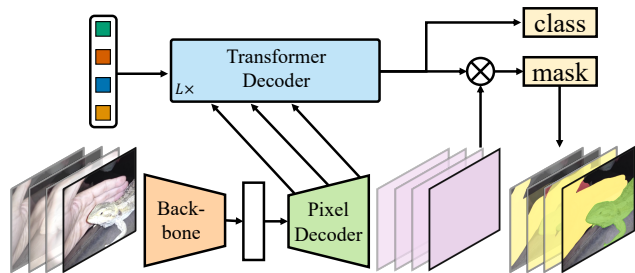


Figure 1. Mask2Former trivially generalizes to videos. For single-frame input data, it operates as a standard image segmentation architecture. For  $> 1$  frames, due to sharing of the queries across frames, it segments and tracks object instances across frames.

dict a 3D volume to track each object instance across time (Fig. 1). This simple change results in state-of-the-art performance of 60.4 AP on the challenging YouTubeVIS-2019 data and 52.6 AP on YouTubeVIS-2021.

## 2. Background

Video instance segmentation (VIS) [18] requires tracking instances across time. In general, there are two ways to extend image segmentation models for the VIS task:

**Per-frame** methods (a.k.a. **online** methods) treat a video clip as a sequence of frames. They run image segmentation models on each frame independently and associate predicted instance masks across frames with a post-processing step. MaskTrack R-CNN [18], TrackR-CNN [14] and VP-SNet [9] add per-instance track embedding prediction to Mask R-CNN [6]. VIP-DeepLab [13] extends Panoptic-DeepLab [3] by predicting instance center offsets across frames. However, it is not always straightforward to modify an image segmentation model, as architectural changes and additional losses are needed.

**Per-clip** methods (a.k.a. **offline** methods) treat a video clip as a 3D spatio-temporal volume and directly predict the 3D mask for each instance. STEM-Seg [1] predicts and clusters spatio-temporal instance embeddings to generate 3D masks. More recently, inspired by the success of DETR [2], VisTR [15], IFC [8] and SeqFormer [16] design

 Work done while Bowen Cheng (bcheng9@illinois.edu) at FAIR.

<sup>†</sup>Equal advising.

Transformer-based architectures to process the 3D volume via cross-attention. However, all these models are designed specifically for video instance segmentation, disconnecting image and video segmentation research. In this report, we show Mask2Former [4], a state-of-the-art universal image segmentation model, can also achieve state-of-the-art video instance segmentation *without* modifying the architecture, the loss or even the training pipeline.

### 3. Mask2Former for Videos

We treat a video sequence as a 3D spatio-temporal volume of dimension  $T \times H \times W$ , where  $T$  is the number of frames and  $H, W$  are height and width respectively. We make three changes to adapt Mask2Former to video segmentation: 1) we apply the masked attention to the spatio-temporal volume; 2) we add an extra positional encoding for the temporal dimension; and 3) we directly predict a 3D volume of an instance across time.

#### 3.1. Joint spatio-temporal masked attention

We apply masked attention to the 3D spatio-temporal features, *i.e.*, we use

$$\mathbf{X}_l = \text{softmax}(\mathcal{M}_{l-1} + \mathbf{Q}_l \mathbf{K}_l^T) \mathbf{V}_l + \mathbf{X}_{l-1}. \quad (1)$$

Here,  $l$  is the layer index,  $\mathbf{X}_l \in \mathbb{R}^{N \times C}$  refers to  $N$   $C$ -dimensional query features at the  $l^{\text{th}}$  layer and  $\mathbf{Q}_l = f_Q(\mathbf{X}_{l-1}) \in \mathbb{R}^{N \times C}$ .  $\mathbf{X}_0$  denotes input query features of the Transformer decoder.  $\mathbf{K}_l, \mathbf{V}_l \in \mathbb{R}^{T H_l W_l \times C}$  are the spatio-temporal features under transformation  $f_K(\cdot)$  and  $f_V(\cdot)$  respectively,  $T$  is the number of frames and  $H_l$  and  $W_l$  are the spatial resolution.  $f_Q, f_K$  and  $f_V$  are linear functions.

Moreover, the 3D attention mask  $\mathcal{M}_{l-1}$  at feature location  $(t, x, y)$  is

$$\mathcal{M}_{l-1}(t, x, y) = \begin{cases} 0 & \text{if } \mathbf{M}_{l-1}(t, x, y) = 1 \\ -\infty & \text{otherwise} \end{cases}. \quad (2)$$

Here,  $\mathbf{M}_{l-1} \in \{0, 1\}^{N \times T H_l W_l}$  is the binarized output (thresholded at 0.5) of the resized 3D mask prediction of the previous  $(l - 1)$ -th Transformer decoder layer.

#### 3.2. Temporal positional encoding

To obtain compatibility with image segmentation models we decouple the temporal positional encoding from the spatial encoding, *i.e.*, we use the positional encoding

$$e_{\text{pos}} = e_{\text{pos-t}} \oplus e_{\text{pos-xy}}. \quad (3)$$

Here,  $e_{\text{pos}} \in \mathbb{R}^{T \times H_l \times W_l \times C}$  is the final positional encoding,  $e_{\text{pos-t}} \in \mathbb{R}^{T \times 1 \times 1 \times C}$  and  $e_{\text{pos-xy}} \in \mathbb{R}^{1 \times H_l \times W_l \times C}$  are the corresponding temporal and spatial positional encodings. Both  $e_{\text{pos-t}}$  and  $e_{\text{pos-xy}}$  are non-parametric sinusoidal positional encodings that can handle arbitrary length.  $\oplus$  denotes addition with `numpy`-style broadcasting.

	method	backbone	data	AP	AP50	AP75
CNN	VisTR [15]	R50	V	36.2	59.8	36.9
		R101	V	40.1	45.0	38.3
	IFC [8]	R50	V	41.2	65.1	44.6
		R101	V	42.6	66.6	46.3
	Mask2Former	R50	V	45.1	66.9	50.5
		R50	V + C80k	47.4	69.8	51.8
		R101	V + C80k	49.0	71.1	<b>55.7</b>
		R50	V	46.4 $\pm$ 0.8	68.0	50.0
Transformer	Mask2Former	R101	V	<b>49.2 <math>\pm</math> 0.7</b>	<b>72.8</b>	54.2
		SeqFormer [16]	Swin-L	V + C80k	59.3	82.1
	Mask2Former	Swin-T	V	51.5 $\pm$ 0.7	75.0	56.5
		Swin-S	V	54.3 $\pm$ 0.7	79.0	58.8
		Swin-B	V	59.5 $\pm$ 0.7	84.3	67.2
		Swin-L	V	<b>60.4 <math>\pm</math> 0.5</b>	<b>84.4</b>	<b>67.0</b>
best of 5 runs	Swin-L	V	60.7	84.4	66.7	

Table 1. **YouTubeVIS-2019 val.** Mask2Former outperforms all state-of-the-art models *without* using image data for augmentation. V: YouTubeVIS-2019 train set. C80k: 80k COCO train2017 images that contain YouTubeVIS categories. We report the median of 5 runs together with the standard deviation.

	method	backbone	data	AP	AP50	AP75
CNN	IFC [8]	R50	V	36.6	57.9	39.3
	SeqFormer [16]	R50	V + C80k	40.5	62.4	43.7
	Mask2Former	R50	V	40.6 $\pm$ 0.7	60.9	41.8
		R101	V	<b>42.4 <math>\pm</math> 0.6</b>	<b>65.9</b>	<b>45.8</b>
Transformer	SeqFormer [16]	Swin-L	V + C80k	51.8	74.6	58.2
	Mask2Former	Swin-T	V	45.9 $\pm$ 0.6	68.7	50.7
		Swin-S	V	48.6 $\pm$ 0.4	77.2	52.0
		Swin-B	V	52.0 $\pm$ 0.6	76.5	54.2
		Swin-L	V	<b>52.6 <math>\pm</math> 0.7</b>	<b>76.4</b>	<b>57.2</b>
	best of 5 runs	Swin-L	V	53.0	75.9	58.4

Table 2. **YouTubeVIS-2021 val.** Mask2Former outperforms all state-of-the-art models *without* using image data for augmentation. V: YouTubeVIS-2021 train set. C80k: 80k COCO train2017 images that contain YouTubeVIS categories. For Swin-L models, we evaluate with a lower resolution (shorter side to 360 pixels) due to memory constraints. We report the median of 5 runs together with the standard deviation.

#### 3.3. Joint spatio-temporal mask prediction

Similarly to the masked attention, we obtain the 3D mask of the  $n^{\text{th}}$  query via a simple dot product, *i.e.*,

$$\mathbf{M}(n, t, h, w) = \text{sigmoid}(\mathbf{E}_{\text{mask}}(:, n)^T \cdot \mathbf{E}_{\text{pixel}}(:, t, h, w)). \quad (4)$$

Note, computation of the classification does not change.

## 4. Experiments

We evaluate Mask2Former on YouTubeVIS-2019 and YouTubeVIS-2021 [18]. We do not modify the architecture, the loss or even the training pipeline.

## 4.1. Training

We use Detectron2 [17] and follow the IFC [8] settings for video instance segmentation. More specifically, we use the AdamW [12] optimizer and the step learning rate schedule. We use an initial learning rate of 0.0001 and a weight decay of 0.05 for all backbones. A learning rate multiplier of 0.1 is applied to the backbone and we decay the learning rate at 2/3 fractions of the total number of training steps by a factor of 10. We train our models for 6k iterations with a batch size of 16 for YouTubeVIS-2019 and 8k iterations for YouTubeVIS-2021. During training, each video clip is composed of  $T = 2$  frames, which makes the training much more efficient (2 hours per training with 8 V100 GPUs), and the shorter spatial side is resized to either 360 or 480. All models are initialized with COCO [10] instance segmentation models from [4]. Unlike [16], we only use YouTubeVIS training data and do not use COCO images for data augmentation.

## 4.2. Inference

Our model is able to handle video sequences of various length. During inference, we provide the whole video sequence as input to the model and obtain 3D mask predictions without any post-processing. We keep the top 10 predictions for each video sequence. If not stated otherwise, we resize the shorter side to 360 pixels during inference for ResNet [7] backbones and to 480 pixels for Swin Transformer [11] backbones.

## 4.3. Results

We compare Mask2Former with state-of-the-art models on the YouTubeVIS-2019 dataset in Table 1 and the YouTubeVIS-2021 dataset in Table 2. Using the exact same training parameters, Mask2Former outperforms IFC [8] by more than 6 AP. Mask2Former also outperforms concurrent SeqFormer [16] without using extra COCO images for data augmentation.

**Acknowledgments:** B. Cheng, A. Choudhuri and A. Schwing were supported in part by NSF grants #1718221, 2008387, 2045586, 2106825, MRI #1725729, NIFA award 2020-67021-32799 and Cisco Systems Inc. (Gift Award CG 1377144 - thanks for access to Arcetri).

## References

- [1] Ali Athar, Sabarinath Mahadevan, Aljosa Osep, Laura Leal-Taixé, and Bastian Leibe. Stem-seg: Spatio-temporal embeddings for instance segmentation in videos. In *ECCV*, 2020.
- [2] Nicolas Carion, Francisco Massa, Gabriel Synnaeve, Nicolas Usunier, Alexander Kirillov, and Sergey Zagoruyko. End-to-end object detection with transformers. In *ECCV*, 2020.
- [3] Bowen Cheng, Maxwell D Collins, Yukun Zhu, Ting Liu, Thomas S Huang, Hartwig Adam, and Liang-Chieh Chen. Panoptic-DeepLab: A simple, strong, and fast baseline for bottom-up panoptic segmentation. In *CVPR*, 2020.
- [4] Bowen Cheng, Ishan Misra, Alexander G. Schwing, Alexander Kirillov, and Rohit Girdhar. Masked-attention mask transformer for universal image segmentation. *arXiv preprint arXiv:2112.01527*, 2021.
- [5] Bowen Cheng, Alexander G. Schwing, and Alexander Kirillov. Per-pixel classification is not all you need for semantic segmentation. In *NeurIPS*, 2021.
- [6] Kaiming He, Georgia Gkioxari, Piotr Dollár, and Ross Girshick. Mask R-CNN. In *ICCV*, 2017.
- [7] Kaiming He, Xiangyu Zhang, Shaoqing Ren, and Jian Sun. Deep residual learning for image recognition. In *CVPR*, 2016.
- [8] Sukjun Hwang, Miran Heo, Seoung Wug Oh, and Seon Joo Kim. Video instance segmentation using inter-frame communication transformers. In *NeurIPS*, 2021.
- [9] Dahun Kim, Sanghyun Woo, Joon-Young Lee, and In So Kweon. Video panoptic segmentation. In *CVPR*, 2020.
- [10] Tsung-Yi Lin, Michael Maire, Serge Belongie, James Hays, Pietro Perona, Deva Ramanan, Piotr Dollár, and C Lawrence Zitnick. Microsoft COCO: Common objects in context. In *ECCV*, 2014.
- [11] Ze Liu, Yutong Lin, Yue Cao, Han Hu, Yixuan Wei, Zheng Zhang, Stephen Lin, and Baining Guo. Swin transformer: Hierarchical vision transformer using shifted windows. *arXiv:2103.14030*, 2021.
- [12] Ilya Loshchilov and Frank Hutter. Decoupled weight decay regularization. In *ICLR*, 2019.
- [13] Siyuan Qiao, Yukun Zhu, Hartwig Adam, Alan Yuille, and Liang-Chieh Chen. Vip-deeplab: Learning visual perception with depth-aware video panoptic segmentation. In *CVPR*, 2021.
- [14] Paul Voigtlaender, Michael Krause, Aljosa Osep, Jonathon Luiten, Berin Balachandar Gnana Sekar, Andreas Geiger, and Bastian Leibe. Mots: Multi-object tracking and segmentation. In *CVPR*, 2019.
- [15] Yuqing Wang, Zhaoliang Xu, Xinlong Wang, Chunhua Shen, Baoshan Cheng, Hao Shen, and Huaxia Xia. End-to-end video instance segmentation with transformers. In *CVPR*, 2021.
- [16] Junfeng Wu, Yi Jiang, Wenqing Zhang, Xiang Bai, and Song Bai. Seqformer: a frustratingly simple model for video instance segmentation. *arXiv preprint arXiv:2112.08275*, 2021.
- [17] Yuxin Wu, Alexander Kirillov, Francisco Massa, Wan-Yen Lo, and Ross Girshick. Detectron2. <https://github.com/facebookresearch/detectron2>, 2019.
- [18] Linjie Yang, Yuchen Fan, and Ning Xu. Video instance segmentation. In *ICCV*, 2019.